Time-dependent density functional study of UV-visible absorption spectra of small noble metal clusters (Cu-n, Ag-n, Au-n, n=2-9, 20)

B. Anak, M. Bencharif, Franck Rabilloud

Time-Dependent Density Functional Study of UV-Visible Absorption Spectra of Small Noble Metal Clusters (Cu_n, Ag_n, Au_n, $n = 2 - 9, 20$)

Berkahem Anak,[1] Mustapha Bencharif,[1] and Franck Rabilloud[2]
[1)] *Laboratoire de Chimie des Matériaux, Université Constantine 1, Constantine, Algérie*
[2)] *Institut Lumière Matière, UMR5306 Université Lyon 1 - CNRS, Université de Lyon, 69622 Villeurbanne Cedex, France*

(Dated: 21 November 2013)

Absorption UV-visible spectra of noble metal clusters Cu_n, Ag_n, Au_n, $n = 2-9$ and 20, are investigated in the framework of the time-dependent density functional theory (TDDFT) using the long-range corrected density functionals LC-M06L and CAM-B3LYP and high-quality gaussian basis sets. Some calculations including the spin-orbit coupling are also presented. The contribution of the d electrons to the optical response is found to be lower than it is when a purely local exchange functional is used. Calculated spectra are compared to experimental ones measured on clusters embedded in rare gas matrix.

Keywords: TDDFT, metal clusters, long-range corrected density functionals, absorption spectra

I. INTRODUCTION

The optical properties of metal nanoparticles is a topic of great fundamental and technological interest. In particular, group-11 element (Cu,Ag,Au) nanoparticles have been intensively studied due to a large potential applicability originating from their unique optical and electronic properties[1]. The size-dependent evolution of the optical properties of noble metal clusters have been the subject of many theoretical and experimental studies for many years. At the nanometric size, the well known plasmonic excitation has been understood as a collective response of valence electrons and can be predicted by classical or semiclassical approaches based on Maxwell's equations for electromagnetic waves interacting with spherical metallic particles characterized by a phenomenological dielectric function[2–5]. In contrast, the optical absorption of small clusters, containing only a few atoms, is molecular-like in the UV-visible range, and can not be described by classical models. A fully quantum treatment for all electrons is required.

Due to their isoelectronic shells (...$3d^{10}4s^1$ for copper, ...$4d^{10}5s^1$ for silver, ...$5d^{10}6s^1$ for gold), the complexity of copper, silver and gold clusters lies between that of alkali metals and transition metals. The presence of d-type electrons strongly affects the physical and chemical properties of clusters. However, several remarkable differences can be found when comparing the three coinage metals. While silver is the most alkali-like transition metal thanks to a relatively large $s-d$ separation, both copper and gold present high $s-d$ hybridization effects. Moreover in the case of gold, relativistic effects and aurophilic interactions[6,7] (closed shell d^{10}-d^{10} interactions) lead to the persistence of planar structures up to at least ten atoms. At atomic level, the energetic position of the nd-levels is approximately 4 eV below the $(n+1)s$ levels in silver, but only about 2 eV in copper and gold. In bulk, the s level are extended to a large band while the atomic d-states develop in a much more localized d-band. The frontier orbital of the d-band is approximately 4 eV below the Fermi energy for silver, but only ~ 2 eV for copper and gold[8]. Consequently, silver presents a strong plasmon absorption in UV-vis domain, visible down to small cluster sizes, followed by interband transitions at higher energies, and in contrast copper and gold have a more complicated absorption because their plasmon band is strongly perturbated by $s-d$ hybridization effects, leading to a scattering of the oscillator strengths over a large energy range. While the optical properties of silver clusters are successfully predicted either by quantum theories for small sizes[9] or by semi-classical approaches at the nanometric size in terms of plasmon excitations, a good description for copper and gold clusters are still challenging due to the active participation of d-electrons in the electronic transitions, and also the spin-orbit coupling in gold clusters, which lead to an high spectral density and an attenuation of oscillator strengths, i.e. a broadening and damping of the optical response.

Experimentally, the optical spectra of small silver cationic Ag_n^+ ($n = 9, 11, 15, 21$) clusters were first obtained by photofragmentation of mass-selected cluster beams[10,11]. Meantime, the first optical absorption measurements of small silver neutral Ag_n ($n = 2-39$) clusters embedded in rare-gas matrix were performed.[12,13] Afterwards, Félix et al have measured optical spectra for even-sized clusters[14]. More recently, Harbich et al have published a new series of absorption measurements on small silver Ag_n ($n = 2-9$) clusters deposited at 6 K in solid neon[15]. The latter, which show much better resolution and structures not present in previous measurements, were suggested by the authors to be taken as benchmark for calculations on neutral silver clusters. For very small Ag_n clusters ($n \leq 8$), the absorption spectra are characterized by a strong response on the 3 - 5 eV range with several narrow or broad peaks, while for $n \geq 12$ they are characterized by the emergence of a dominant and relatively broad peak between 3 and 4 eV, somewhat similar to the well known surface plasmon resonance observed at the nanometric size. Theoretically, the observed spec-

tra for silver clusters were first interpreted using classical electrodynamics by solving Maxwell's equations for electromagnetic waves interacting with small spherical metallic particles (Mie theory), or ellipsoidal particles (Mie-Gans theory), characterized by the dielectric function of the bulk[13,16]. In these classical or semiclassical theories, the plasmon resonance reflects a collective excitation of the s valence electrons, while the effects of the d-electrons were only accounted for by using the bulk dielectric function. More recently, a few studies[9,14–21] have been performed within a fully quantum treatment for all electrons in the framework of the time-dependent density functional theory[22–24] (TDDFT) on silver clusters of some tens of atoms.

The strong $d-s$ hybridization and relativistic effects of gold lead to very rich absorption spectra in the UV-visible domain. A variety of techniques such as inert gas complex beam depletion spectroscopy[25–27], photoelectron spectroscopy[28], and more recently the photodissociation spectroscopy[29,30] and noble-gas matrix spectroscopy[8], have been used to measure the optical response of small neutral or charged gold clusters. Describing the optical absorption of gold clusters is difficult because of relativistic effects, including the spin-orbit contribution[31], and the strong influence of d-electrons. Contrary to silver atoms, where the relatively large $s-d$ separation makes the optical response mainly associated to s-electrons, the small $s-d$ separation in Au atoms leads to the active participation of d-electrons in the electronic transitions, attenuating oscillator strengths. A few previous works have been performed in the framework of TDDFT using several levels of approximations: the local density approximation[32,33] (LDA), the GGA-type (generalized gradient approximations) density functional[34], the hybrid functionals B3LYP[15,26,27,29], the LB94 density functional[35], and more recently some long-range corrected functionals[36]. Calculations with the wave function excited-states method equation-of-motion coupled cluster singles and doubles (EOM-CCSD) have also been performed for Au_4 and Au_8[36]. However, none of these calculations are in satisfactory agreement with the experimental spectra of neutral clusters.

To our knowledge, very few studies have been published on absorption spectra of copper clusters. Recently, Harbich[37] measured the optical absorption of small Cu_n ($n=1-9$) clusters in neon matrix at 7 K. Theoretically, TDDFT calculations using LDA[38] or GGA[39] or B3LYP[37] density functionals do not reproduce very well the experimental data. Calculations are somewhat difficult due to $s-d$ hybridization effects and interband transitions.

We present here new TDDFT calculations of absorption spectra of Ag_n, Au_n, Cu_n with $n=2-9,20$. Calculations have been performed in the adiabatic linear-response formulation using several long-range corrected (LC) density functionals with an high-quality gaussian basis set. Contrary to standard GGA-type density functionals which suffer from the self-interaction error (SIE) resulting in an incorrect asymptotic behavior of the exchange-correlation potential, the LC density functionals restore the correct asymptote by introducing a range separation into the exchange component by splitting the Coulomb operator into short-range and long-range parts. While the short-range part is still evaluated with the exchange potential from DFT, the long-range term is evaluated with the Hartree-Foch exchange to eliminate or decrease the long-range SIE[40,41]. Recently the use of such functionals was showed to give significant improvements concerning the prediction of absorption spectra of metal clusters[9,36]. In particular, the analysis has showed that the $d \rightarrow sp$ interband transitions present a long-range charge-transfer character with a relatively low overlap between occupied and virtual orbitals and a significant blue shift induced by the Hartree-Fock exchange. These interband transitions are properly described only with a correct asymptotic potential[9].

We will present new analysis based on TDDFT with LC density functionals that will allows us to characterize the transitions for the group-11 element (Cu,Ag,Au) clusters and compare the role of the d electrons in the three metals. We also present TDDFT calculations including spin-orbit coupling. To our knowledge, the present calculations are the first ones concerning noble metal clusters which take into account the spin-orbit coupling at a such high level of theory. Our results will be compared with experiments when available.

II. COMPUTATIONAL DETAILS

Both silver and gold atoms were described through a relativistic effective core potential (RECP) so that only 19 valence electrons were treated explicitly[42]. The def2-QZVP basis sets was used for all atoms[43], it was (24s18p10d3f1g)/[11s6p5d3f1g] for Cu, (10s8p7d3f1g)/[7s5p4d3f1g] for Ag and (9s8p6d3f1g)/[7s5p4d3f1g] for Au. However, in cases of Cu_{20}, Ag_{20} and Au_{20}, a smaller basis set (hereafter called SDD) by Andrae et al[42] were used in order to reduce the computational time. Two exchange and correlation density functionals were used: LC-M06L and CAM-B3LYP. LC-M06L is obtained by applying a long-range correction[41] to the meta-GGA M06L[44] functional ("meta" denotes the inclusion of kinetic energy density, which depends on local derivatives of the spin orbitals). LC-M06L contains 0% Hartree-Fock exchange at short range and 100% at long range. The range separation parameter was 0.47. CAM-B3LYP[45] is a long-range corrected hybrid density functional which combines the hybrid B3LYP[46,47] functional at short range with an increasing amount of exact Hartree-Fock at long range. It comprises of 19% Hartree-Fock at short range and 65 % at long range. Calculations were performed with the Gaussian09 suite of programs[48]. Pre- and postprocessing operations were performed by using the graphical interface Gabedit[49]. For small clusters ($n=2-9$) the structures were taken from previous

works[14,50–52]. When several isomers were found to be compete for the ground-state, the absorption spectrum was calculated for all of them. The structure of Ag_{20} was the lowest-energy isomer found in our previous work[14] at DFT/BP86 level, that of Cu_{20} was the lowest-energy isomer obtained in a global optimization[51]. Finally, the well known T_d symmetry structure was considered for Au_{20}. In all cases, the clusters were locally optimized with each functional before doing the present calculation of optical properties.

We have also performed some calculations taking into account the spin-orbit coupling. They were performed using the program ADF[53] in the framework of the zeroth order regular approximation (ZORA) to the Dirac equation[54,55]. Unfortunately, the spin-orbit coupling operator can not be applied with the full kernel of an hybrid functional in the current version of ADF. Accordingly, we have calculated the spin-orbit coupling within the statistical averaging of model orbital potential (SAOP)[56]. The potential SAOP which displays the correct asymptotic behavior has been specifically designed for calculating optical properties. It has yielded very good results for response properties on gold dimer[31]. In our calculations, the spin-orbit coupling was explicitly included into the SCF process for small clusters, but for Au_{20} in order to reduce the computational cost we first performed scalar relativistic TDDFT calculations to determine the lowest singlet-singlet and singlet-triplet excited states and then the spin-orbit coupling operator was applied to these single-group excited states to obtain the excitation energies.

All spectra presented in the figures below give the oscillator strength as a function of the excitation energy, together with a curve obtained by a Gaussian broadening with a full width of half-height of 0.08 eV.

III. RESULTS

A. Absorption Spectra of Silver Ag_n ($n = 2 - 9$) Clusters

Absorption spectra of silver clusters Ag_n, with $n = 2 - 9$, are shown in Figure 1 together with the geometrical structures. Both LC-M06L and CAM-B3LYP spectra are in very good agreement with experimental results measured on cluster embedded in neon matrix at 6 K[15]. Present calculated spectra are somewhat similar to previous ones calculated using CAM-B3LYP with a lower-quality basis set[9,19]. They are of better quality than previous BP86[14], PBE[57] or B3LYP[15] predictions. As expected, spectra of open-shell clusters (odd-sized clusters) present many more transitions than those of closed-shell clusters (even-sized clusters), with the exception of Ag_7 for which the number of transitions is low due to its D_{5h}-symmetry structure. Similarly, calculated spectra of Ag_6 and Ag_8 are found to present very few transitions due to their high symmetry. In the case of Ag_3, the first transition at 2.5 eV is well reproduced both functionals. But at higher energy range, the CAM-B3LYP calculation seems to better reproduce the experimental results than LC-M06L does thanks to two large transitions at 3.42 and 3.65 eV. However no transition is found near 4 eV at CAM-B3LYP level where as the two transitions at 3.89 and 4.02 eV from the LCM06L spectrum fit well the experiment. For Ag_4, CAM-B3LYP gives five main peaks at respectively 3.00, 4.01, 4.42, 5,42 and 5.68 eV, while LC-M06L presents strong transitions at 3.05, 4.00, 4.26, 4.76 and 5.71 eV respectively. In experiment, while two main strong transitions at 3.07 and 4.23 eV can be easily extracted from the spectrum reported in Figure 1, others peaks are identified in the original work[15]. For Ag_5, the two main transitions calculated at 3.24 and 3.63 eV with CAM-B3LYP and 3.30 and 3.74 eV with LC-M06L compare well with the experimental peak located at 3.27 and 3.69 eV respectively. Both functionals give a strong transition near 5 eV (4.91 eV at with CAM-B3LYP and 4.95 eV at LC-M06L level) which could correspond to the experimental transition observed at 5.36 eV. The experimental spectrum of Ag_6 shows a main peak at 3.45 eV with a second less intense one at 3.65 eV. The former is well reproduced by CAM-B3LYP (3.43 eV) and is slightly overestimated by LC-M06L (3.61 eV). But the small peak is shifted on the low-energy side of the main transition at 2.91 eV and 3.09 eV for CAM-B3LYP and LC-M06L respectively. For Ag_7, spectra calculated with the D_{5h}-symmetry structure are in good agreement with the experiment since both the main and secondary peaks are well reproduced. Indeed, the main peak calculated at 3.61 and 3.71 eV at CAM-B3LYP and LC-M06L level respectively is in agreement with the experimental peak at 3.64 eV. Beside the less-intense transitions measured at 2.78 eV and 4.63 eV seem to correspond to the calculated transitions calculated at 2.65 and 4.33 eV at CAM-B3LYP level, and 2.91 and 4.44 eV at LC-M06L level. For Ag_8, two structures of symmetry T_d and D_{2d} respectively compete for the lowest-energy isomer. In the present study, the D_{2d} structure is found to be the lowest-energy isomer at LC-M06L level since it lies 0.03 eV below the T_d structure. In contrast, using CAM-B3LYP the T_d isomer is found to lie 0.17 eV below the D_{2d} structure. The experimental spectrum presents two small narrow peaks at 3.12 and 3.20 eV and two intense transitions at 3.65 and 4.00 eV. Three transitions (at 3.12, 3.20 and 4.00 eV) could correspond to transitions calculated for the T_d isomer at the LC-M06L level (3.02, 3.36 and 4.03 eV) or at the CAM-B3LYP level (3.18 and 3.97 eV). The two experimental peaks at 3.65 and 4.00 eV are well reproduced by transitions calculated for the D_{2d} isomer at 3.74 and 4.03 eV (LC-M06L) and 3.65 and 3.97 eV (CAM-B3LYP). As previously suggested[14], both isomers could be likely present in the experiment, the experimental spectrum being then a sum of the spectra for both isomers. In this context, the energy gap of 0.03 eV calculated at LC-M06L level may appear to be more appropriated than the value of 0.17 eV obtained with CAM-B3LYP which seems to be too large. For Ag_9, the

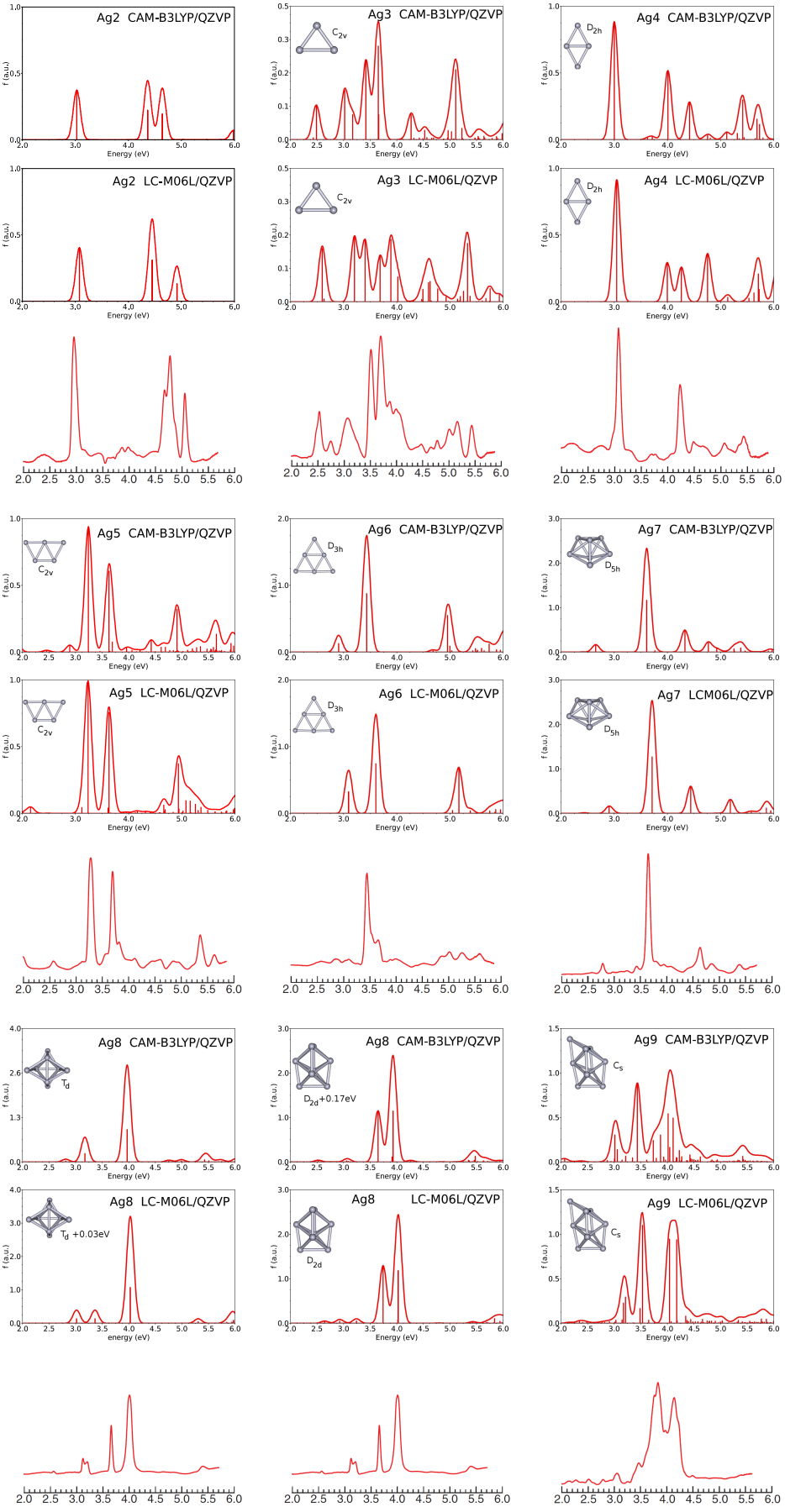

FIG. 1. Calculated absorption spectra of silver clusters Ag_n, with $n = 2 - 9$, compared to experimental spectra measured on clusters embedded in neon matrix. Plot of the experimental spectra (third row for each cluster size) were generated using digitizing software on the original spectra[15].

experimental spectrum in neon matrix shows two main bands at 3.84 and 4.14 eV. It differs from that measured previously in argon matrix where a broader structure composed of several narrow peaks between 3.3 and 4.25 eV were found[14]. In the present work, we have only considered the C_s-symmetry structure shown in Figure 1, as it was found to be lowest energy-isomer in several previous works[14,15]. Calculated absorption spectra are not in perfect agreement with the experiment one. However the analysis of several previous calculations[14,58] indicate that different structures have minimum energies in an energy range as close as 0.05 eV, and so the observed spectrum could be the sum of contributions from several isomers present inside the matrix as already examined in a previous study[59].

B. Absorption Spectra of Copper Cu_n ($n = 2-9$) Clusters

Recently, the optical absorption of small Cu_n clusters embedded in neon matrix at 7 K have been measured[37]. Afterwards, TDDFT calculations using LDA[38] and B3LYP[37] density functionals were found to be not able to well reproduce the experimental data. Present work, with the use of long-range density functionals and an extended basis set, represents a significant improvement over previous theoretical studies since the $d \rightarrow sp$ interband transitions which may present a significant long-range charge-transfer character[9] will be better described. Calculated absorption spectra are given in Figure 2 together with the experimental ones (see also Supplementary Information for the spectrum of a second isomer of Cu_3). Our results are in better agreement with the experiment than those obtained at TDLDA and TDDFT/B3LYP levels, especially for $n = 2$,3 and 8. As expected, the number of transitions is strongly reduced when the long-range correction is added. For example the number of states below 5 eV is divided by a factor of 2 when using CAM-B3LYP instead of the B3LYP density functional. However our absorption spectra can not clearly account for the measured spectra since the detailed structures are only partially reproduced.

For the dimer, the measured peaks at 2.80, 4.68, 5.08, 5.41 eV could correspond to the calculated transitions at 2.89, 4.45, 5.19, 5.42 eV with CAM-B3LYP and 2.94, 4.56, 5.41, 5.76 eV at LC-M06L level. For the trimer, a qualitative agreement can be found at least at low energy where calculations furnish strong transitions close to 2.5 eV and 3.5 eV. For Cu_4, the spectrum calculated at LC-M06L level is slightly blueshifted in comparison with that obtained with CAM-B3LYP level. But both calculated spectra give a main transition at about 3 eV and a second one in the 4.5-5 eV range, while none of them reproduce the experimental peaks in the 3.5-4 eV range. For Cu_5, the two calculated spectra are very similar, they show one main transition centered at 3.22 and 3.37 eV with CAM-B3LYP and LC-M06L respectively. For Cu_6, Cu_7, Cu_8, the calculated spectrum with CAM-B3LYP is somewhat similar to that obtained at LC-M06L level. The correspondence with the experiment is not good for Cu_6 and Cu_7, but it is better for Cu_8.

C. Absorption Spectra of Gold Au_n ($n = 2-9$) Clusters

The optical properties of small gold clusters have been the object of many works. Among them, several studies in the framework of TDDFT have been published[8,32,33,36] But the recent work by Chalasinski et al[36] on even-sized clusters is the only one considering long-range corrected density functionals, while the previous works used LDA or B3LYP density functionals. Figure 3 shows our calculated absorption spectra together with the experimental ones measured on clusters embedded in neon matrix at 7 K (see also Supplementary Information for spectra of higher-energy isomers). Planar structures are also given in the figure. In experiment, absorption spectra are characterized by a very rich response and with a high density of transitions in all the 2-6 eV range. Calculated spectra also present a high density of states, especially for open-shell systems ($n = 3, 5, 7, 9$). For dimer, the two calculated spectra are similar with two transitions at 2.97 and 5.53 eV at CAM-B3LYP compared to 3.13 and 5.57 eV with LC-M06L. Significant differences can be found in spectra calculated for trimer and tetramer. For the trimer, the first strong transition is calculated at 2.54 eV with CAM-B3LYP and 3.36 eV with LC-M06L. For Au_4, two main transitions are found around 3 eV (at 3.03 and 3.21 eV) with CAM-B3LYP, while only one exists with LC-M06L (at 3.26 eV) but with a much stronger oscillator strength. For Au_5, Au_6, Au_7 and Au_8, spectra calculated with both functionals are somewhat similar, while several transitions calculated at LC-M06L level are slightly blueshifted when comparing to those obtained at CAM-B3LYP level. For Au_9, many transitions give rise to a continuum spectrum starting from 2.5 eV.

To compare the calculated and experimental spectra is not so easy because the high density of transitions leads the shape of the calculated spectrum strongly dependent on the arbitrary gaussian broadening. However, the measured spectra show many transitions in the 2-6 eV range, generally starting from 2 eV. Unfortunately the first allowed transitions in calculated spectra appear at higher energy. Clearly, the calculated absorption spectra do not reproduce the experimental spectra below 3 eV. However, calculations show symmetry forbidden transitions in the 2-3 eV range that could possibly explain the measured peaks, if they can be observed when the cluster is embedded due to the interaction with the rare-gas atoms.

D. Absorption Spectra of Ag_{20}, Cu_{20} and Au_{20}

Figure 4 gives the calculated absorption spectra of clusters of size $n = 20$. For the three metals, the spectrum is characterized by a strong plasmon-like band in the 3.5-

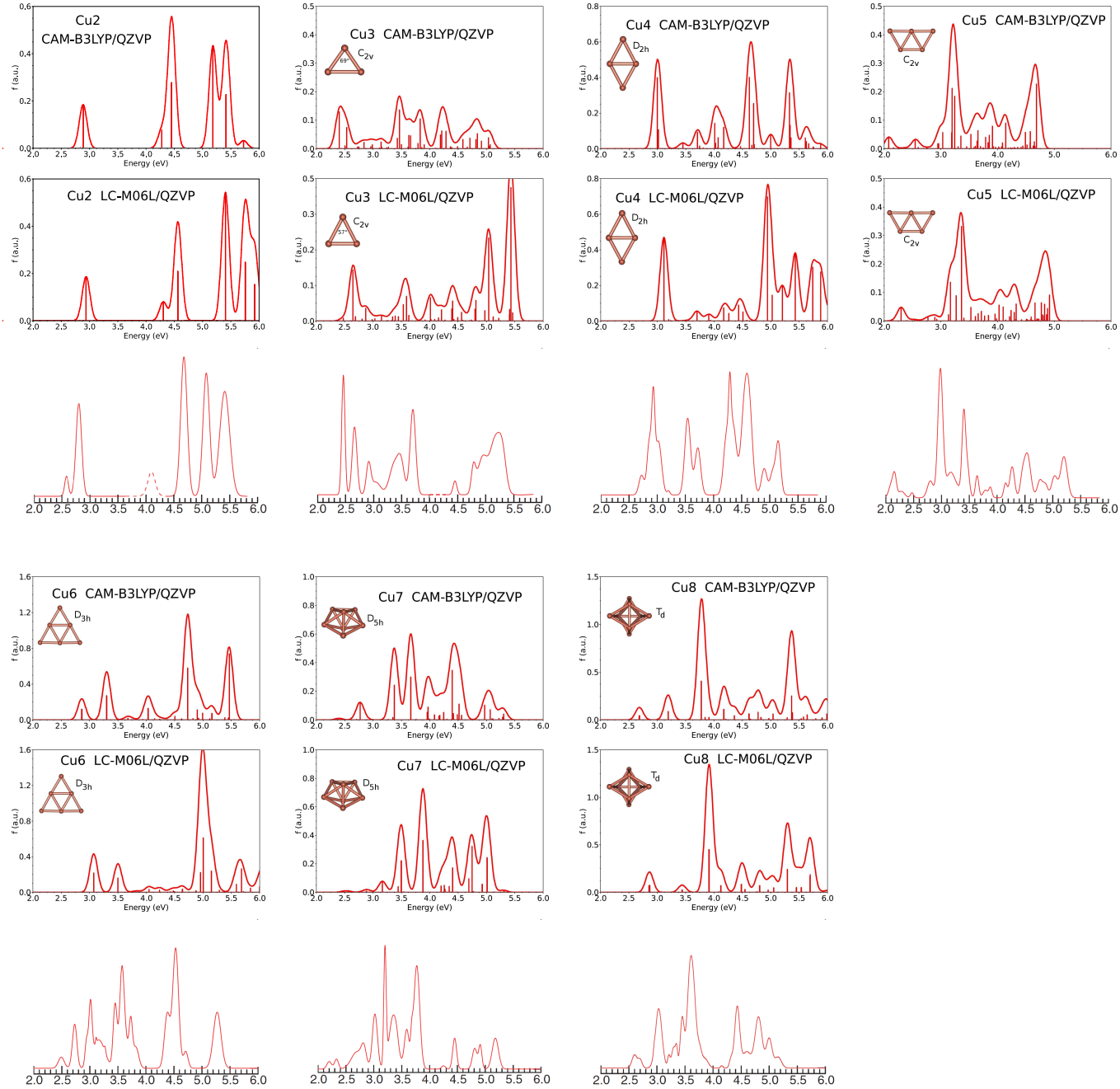

FIG. 2. Calculated absorption spectra of copper clusters Cu_n, with $n = 2 - 8$, compared to experimental spectra measured on clusters embedded in neon matrix. Plot of the experimental spectra (third row for each cluster size) were generated using digitizing software on the original spectra[37].

4 eV range. For silver, the band is centered at 3.88 and 4.09 eV at CAM-B3LYP and LC-M06L levels respectively, then no transition is found up to 6 eV. For copper, the plasmon band is calculated at 3.70 eV and 4.00 eV with CAM-B3LYP and LC-M06L respectively, followed by a large band starting at 4.5 or 5.0 eV depending on the functional used. Some low transitions are also visible before the plasmon band. The oscillator strength associated to the plasmon-like band is much less intense than it does for silver. Finally, for Au_{20} the plasmon-like band is associated to an unique transition due to the high symmetry of the structure (T_d), it is located at 3.47 eV at CAM-B3LYP level and 3.80 eV at LC-M06L level. Moreover, two weak peaks at low energies are also found respectively at 2.70 and 3.16 eV with CAM-B3LYP, and at 2.97 and 3.50 eV at LC-M06L level. Our results are in good agreement with the recent work by Koppen and al[60] in which several families of density

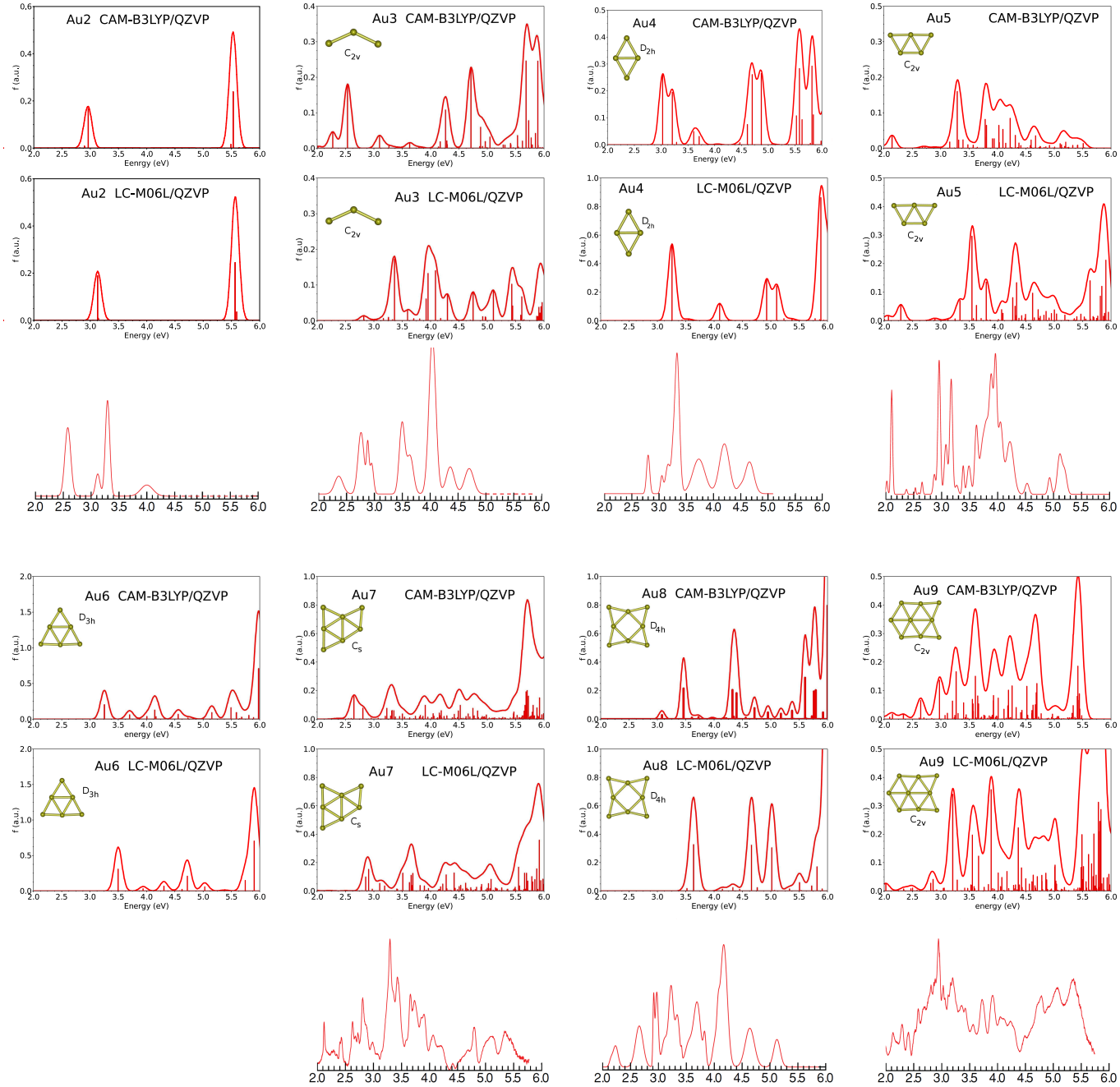

FIG. 3. Calculated absorption spectra of gold clusters Au_n, with $n = 2 - 9$, compared to experimental spectra measured on clusters embedded in neon matrix. Plot of the experimental spectra (third row for each cluster size) were generated using digitizing software on the original spectra[8].

functionals were tested on Au_{20} clusters. In particular, the global hybrid ωB97x density functional were found to give a strong transition at 3.57 eV and two less-intense peaks at 2.93 and 3.37 eV. In contrast, LDA and GGA predictions produce peaks at much lower energies[32,33,61]. LDA calculation[33] predicts a weak transition at 1.85 eV and a strong one at 2.78 eV, while BP86 calculation[61] finds some transitions at 1.90 and 2.89 eV.

E. Spin-Orbit Coupling

In all above TDDFT calculations, the relativistic corrections for gold and silver were accounted for at a scalar level through the use of a RECP. This was essential, specially in the case of gold for which the relativistic effects lead to a quenching of the oscillator strength due to enhanced screening of the s electrons by the d electrons and the strong $s - d$ hybridization in the low en-

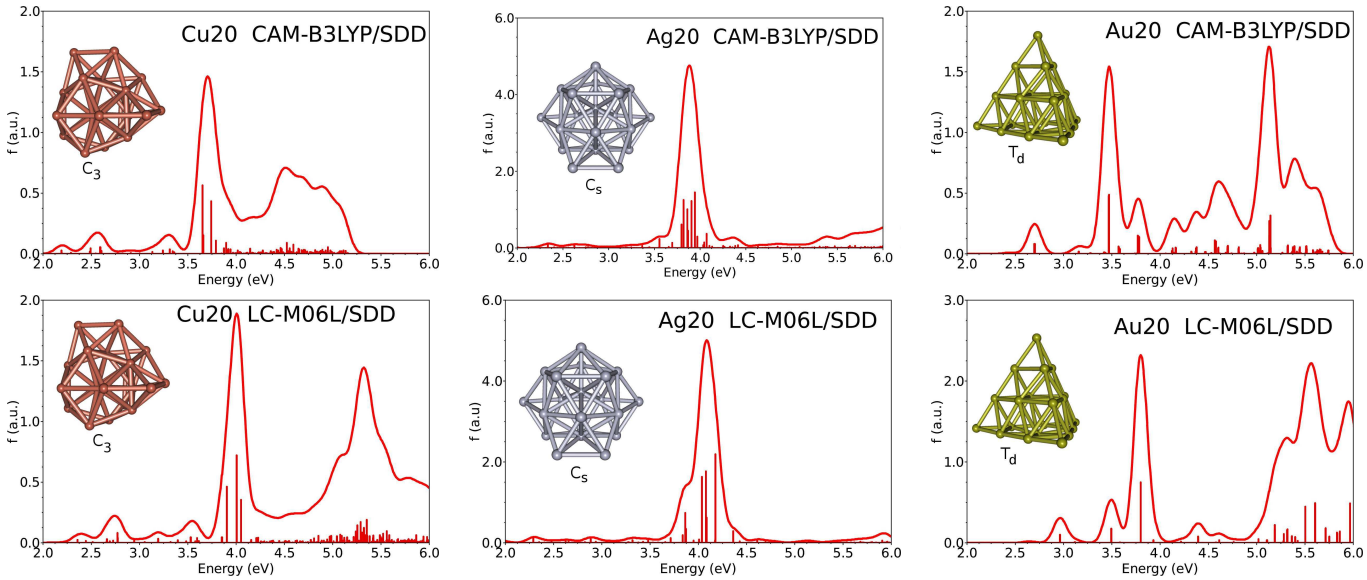

FIG. 4. Calculated absorption spectra of Cu_{20}, Ag_{20} and Au_{20}.

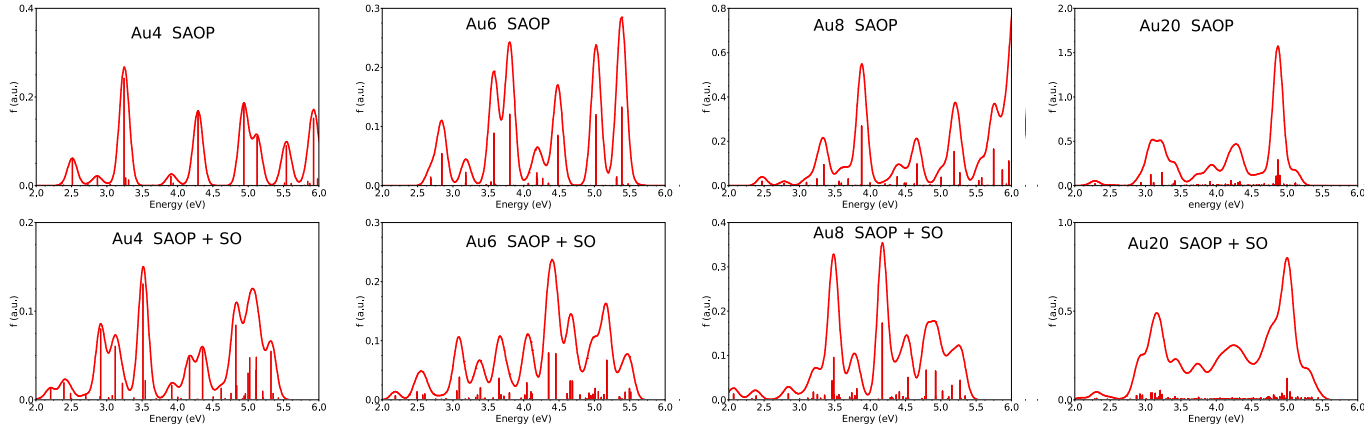

FIG. 5. Calculated absorption spectra of Au_n clusters with $n = 4, 6, 8, 20$ using the SAOP method without and with the spin-orbit (SO) coupling. Structures of clusters are shown in Figures 3 and 4. Other spectra for silver and copper clusters are available in Supplementary information.

ergy transitions. However, the above calculations neglect the effects of spin-orbit (SO) coupling. While the latter is expected not to be prominent in copper and silver, it may play a significant role in gold. Recently, Geethalakshli et al[31] have presented an new interpretation of the absorption and emission spectra of the gold dimer showing the significant role of the spin-orbit coupling. They used both *ab initio* multiconfigurational hamiltonian (like a CASSCF/CASPT2 scheme: complete active space self-consistent field followed by second order perturbation theory) and TDDFT framework to generate a space of excited states on which the spin-orbit coupling operator was applied. Their benchmarking among the different methods has shown that the SAOP functional in the case of TDDFT gives good excitation energies and has approximatively the same accuracy along with the *ab initio* methods. Following their work on gold dimer, we have have performed additional calculations in order to investigate the SO coupling in noble metal clusters using TDDFT with the SAOP potential. Figure 5 gives the calculated spectra for closed-shell gold clusters. We have included both spectra obtained at SAOP level without SO coupling and spectra after applying the SO coupling operator. Applying the SO coupling operator leads to several changes in spectra of small clusters including shifts of some main peaks and specially a dispersion of the oscillator strengths resulting into a broadening and damping of the optical response. However, the inclusion of SO coupling does not explain the strong transitions measured at low energies in experiment[8] (for examples transitions at 2.23, 2.66, 2.91, 2.97 eV for Au_8, see Figure 3). Interestingly, the SO coupling effects on the spectrum of Au_{20} are small, since only a small broadening coupled to a small damping is visible but without any changes in

the shape of the spectrum. Hence the SO coupling effects appear to be less important for large systems than for small ones.

In Supplementary information, we furnish spectra of silver and copper clusters calculated with the SAOP potential and SO coupling. As expected, no significant effect of SO coupling can be observed.

IV. DISCUSSION

A. Orbital Character of the Optical Excitations

In order to quantify the respective contributions of s and d electrons to the optical response, we have calculated the percentage of the d character in the transition thanks to the formula proposed by Baishya[16]:

$$\%d = \frac{\sum\limits_{n,\Omega_n<E_c} f_n \sum\limits_{vc} |F_n^{vc}|^2 |\langle d|\phi_v\rangle|^2}{\sum\limits_{n,\Omega_n<E_c} f_n} \times 100, \qquad (1)$$

where the sum in n includes all the excitations up to a cutoff energy E_c. For one transition labelled n with an energy Ω_n and an oscillator strength f_n, the double index vc labels the entries of the corresponding TDDFT eigenvector F_n, which is composed of occupied-unoccupied (or "valence-conduction") Kohn-Sham orbital pairs. Of course $\sum_{vc} |F_n^{vc}|^2 = 1$ for each transition n. $\langle d|\phi_v\rangle$ is the d projection of the occupied orbital ϕ_v. We show in Figure 6 the degree of the integrated d character of the excitations as a function of the cutoff energy E_c. The graphs reported in Figure 6 was calculated at CAM-B3LYP level, similar results were obtained with LC-M06L. The d character in silver is found to be low, about 10% up to $E_c = 5$ eV and about 20 % when $E_c = 6$ eV. The transitions are mainly associated to excitations from s-type orbitals. The excitations from d type orbitals are effective at higher energies. This contrasts with previous TDLDA studies which predicted a much more important contributions of the d electrons to the excitations (50-70% depending on the cluster size[16]). Recently, the purely local functionals were showed to overestimate the role of d electrons in the plasmon-like band of silver Ag_{20} clusters[9], present results show that they also overestimate the role of the d electrons in the optical response of very small clusters. In the case of Ag_{20} our analysis shows that the contribution of the d electrons rises above 5 eV.

As expected, the d character in the excitations is much larger for copper and gold than it is for silver. The d character monotonously rises with the cutoff energy for all copper and gold clusters from about 20% at 3 eV to 60% at 6 eV. The behavior for tetramers somewhat differs since it increases from 50% at 3 eV to about 70 % at 6 eV. The important role of the d electrons in optical properties of copper and gold clusters was already known and explained by considering the relative proximity of the d and s levels and the strong $s-d$ hybridization. In TDLDA calculations, the percentage of d character was found to be at about 80% and 70 % for copper and gold clusters respectively with a cutoff energy of 6 eV [38]. In particular, the d character was large even at low energies ($\sim$ 2 eV). For example, the d character was found to be about 50 % for $E_c = 2$ eV in the case of Cu_{10}. Again, the use of the Hartree-fock exchange at long-range reduces the role of the d electrons in the excitations at low energies.

In the top of the Figure 6, we also give for the size $n = 20$ the evolution of the d character of the integrated excited states as a function of a cutoff energy. It differs from the equation 1 since it includes both white and black states while equation 1 only consider white states (oscillator strength $f_n \neq 0$). The curves show that the d band opens at about 5.1 ev for Ag_{20} and 3.85 eV for Cu_{20} and only 3.75 eV for Au_{20}.

B. Limitations in the experiment - theory comparison

Several hypothesis can be emitted to explain the relative disagreement between experimental and theoretical spectra for copper and gold clusters. We would like to briefly discuss the following two points: the effects of the matrix which are not taken into account in the calculation, and the limitations of TDDFT in the adiabatic linear-response formulation.

First, TDDFT calculations are performed in gas phase where as measurements are made on clusters embedded in rare gas matrix. Although condensed rare-gases are the most inert solids, some effects on spectra may be expected. For example, it was shown on both potassium and silver clusters that the dielectric screening for the electron-electron interaction involve a redshift of the plasmon frequency as the dielectric constant of the matrix increases[62]. Based on the classical Mie approach, Fedrigo et al.[13] have estimated that the plasmon-like band in silver clusters was likely to be redshitfed by 0.24 eV when the clusters are embedded in argon matrix with respect to the gas phase. In the same way, they calculated a redshift of 0.32 and 0.42 eV in krypton and xenon matrices. More recently, the matrix effects of rare gas matrix on spectra of small silver clusters (Ag_n, $n = 2, 4, 6, 8, 20$), were estimated using an electrostatic model of solvation (the well know conductor-like screening model of solvation (COSMO) model) in TDDFT/GGA calculations[63]. An average redshift of 0.17, 0.30, and 0.33 eV of the main peaks in argon, krypton, and xenon matrix respectively was obtained. However, the previous model neglects all nonelectrostatic effects which are likely to be important for rare gases.

The matrix effects do not only cause a shift of the main peaks. Clusters with differing local environments, known as site isomers, may coexist. Using quantum calculations on sodium clusters embedded in an argon matrix, Gervais et al[64,65] showed the possible coexistence of several site

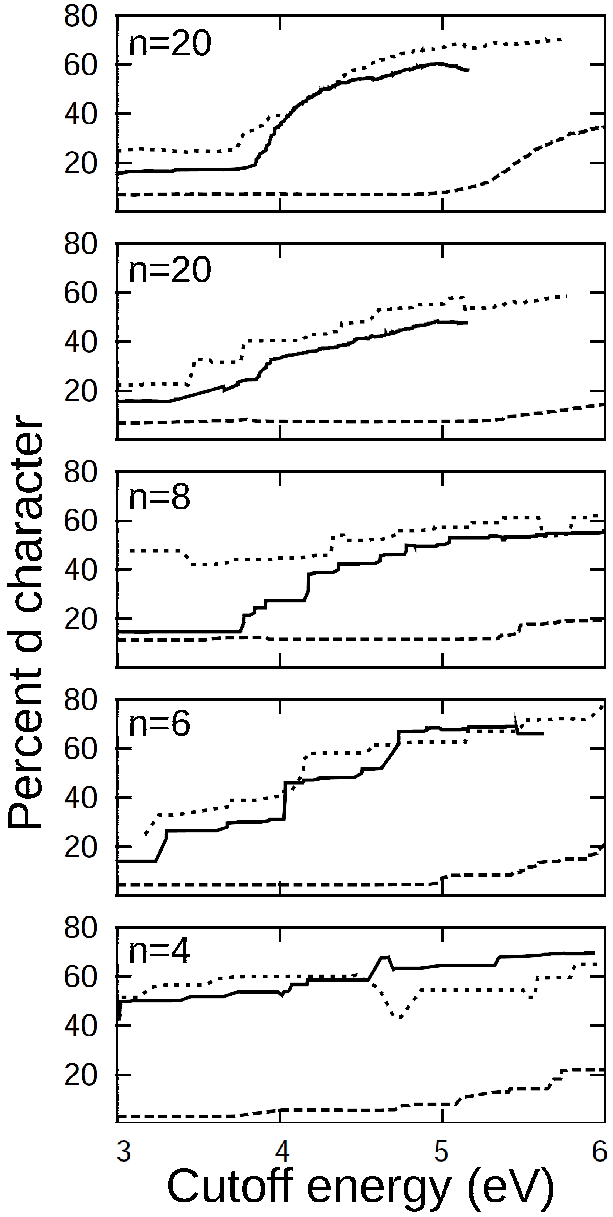

FIG. 6. The percentage of the d character in the optical transitions for Cu_n (solid lines), Ag_n (dashed lines) and Au_n (dotted lines) clusters ($n = 4, 6, 8, 20$) evaluated with the equation 1. The figure on the top gives the d character of excited states for $n = 20$, it differs from that given just below since it includes both black and white excited states, while the other curves are calculated in considering only white states (oscillator strength $f_n \neq 0$)

isomers and rationalized the matrix effects in two competing effects: the dielectric effect leading to a redshift and a confinement of the valence electrons of the clusters due to the presence of the rare-gas atoms leading to a blueshift. Other possible effects concern the eventual deformations of clusters during the deposition in matrix, though the deposition energy is low. Finally, some symmetry forbidden transitions may be observed when the cluster is embedded due to interaction with the rare-gas atoms. To reduce the matrix effects both the growth of the matrix and measurements of optical spectra are made at low temperature (6 or 7 K). In the case of silver, the good agreement between theoretical and experimental spectra yields to conclude that the matrix effects are small. Contrarily, in the case of copper, the failure of the calculations to reproduce experimental results obtained in matrix leads to suppose some significant effects of matrix. However, the structure of clusters is not here necessarily a causal factor for the deformation since both copper and silver clusters have the same structures. The interaction with the neighboring rare atoms may cause significant perturbation in the optical properties of copper clusters.

In the case of gold, the transitions measured at low

energies (below 3 eV) are not observed in our TDDFT calculations in gas phase, even when a spin-orbit coupling operator is applied. The planar structures are expected to be more sensitive to the environment the three-dimensional ones. And transitions measured at low energies may be due to some matrix effects which could either slightly distort the cluster or just break down the symmetry and then make that some black states become visible in matrix. Further calculations including both the spin-orbit coupling and matrix effects are in progress in our group.

We should also mention that the current TDDFT calculations in the adiabatic linear-response formulation are not able to correctly describe states with substantial multi-excitation character. That may be a severe limitation for describing some excited states of copper and gold systems. However, Geethalakshli et al[31] have shown that TDDFT/SAOP and CASPT2 methods give somewhat similar excitation energies in the case of Au_2. Further calculations based on multi-configuration theories would help to confirm the present predictions.

V. CONCLUSIONS

In this work we performed TDDFT calculations of the optical spectra of group-11 elements clusters Cu_n, Ag_n, Au_n, with $n = 2 - 9$ and 20, using the long-range corrected density functionals LC-M06L and CAM-B3LYP with high-quality gaussian basis sets. LC-M06L and CAM-B3LYP spectra are found to be somewhat similar but several main peaks calculated at LC-M06L level are found to be slightly blueshifted in comparison with their corresponding CAM-B3LYP position. This blueshift is connected to the value of the range separation parameter (0.47 in the present work). Very recently, a value of 0.33 was found to give slightly better results on silver clusters[9].

The three noble metal present a strong optical response in the UV-visible range, but some significant differences were found in spectra when comparing the three metal. Silver presents a few strong peaks well separated, while copper and gold furnish spectra with a high density of peaks resulting into a broadening and a damping of the optical response. For the size $n = 20$, the plasmon-like band is calculated in the 3.5-4 eV range for the three metals. However, while no transition is found around it in the case of Ag_{20}, a few transition in found below the plasmon and a large band is found beyond $\sim 4.5-5.0$ for both Cu_{20} and Au_{20}. The contribution of the d electrons to the optical response was found to be much lower than it is at LDA or GGA levels. Applying the spin-orbit coupling leads no significant effects on the spectrum of Au_{20}, but it leads to several changes in spectra of small gold clusters like shifts of several main peaks and specially a dispersion of the oscillator strengths resulting into a broadening and damping of the optical response. As expected, no significant effects of the spin-orbit coupling could be observed on silver and copper clusters.

Our calculated spectra were compared to recent experimental ones measured on clusters embedded in neon matrix at very low temperature (at 6 or 7 K). For Ag_n, our calculated spectra reproduce well the experimental ones. For copper, the comparison is not so good since the detailed structure of spectra is only partially reproduced. For gold clusters, the measured transitions at low energies (below about 3 eV) are not found in our calculations, even when the spin-orbit coupling is included. We discussed the possible effects of the matrix which could cause the occurrence the new peaks not visible in the gas phase.

ACKNOWLEDGMENTS

The authors thank Mingli Yang for providing the initial coordinates of copper clusters. This work was granted access to the HPC resources of IDRIS under the allocation 2013-i2013086864 made by GENCI, and to the HPC resources of PSMN (Pôle Scientifique de Modélisation Numérique).

[1] M. C. Daniel and D. Astruc, *Chem. Rev.*, 2004, **104**, 293.
[2] V. V. Kresin, *Phys. Rev. B*, 1995, **51**, 1844.
[3] L. S. ans A. rubio, *Phys. Rev. Lett.*, 1997, **78**, 1428.
[4] J. Lermé, *Eur. Phys. J. D*, 2000, **10**, 265.
[5] M. Gaudry, J. Lermé, E. Cottancin, M. Pellarin, J. L. Vialle, M. Broyer, B. Prével, M. Treilleux and P. Mélinon, *Phys. Rev. B*, 2001, **64**, 085407.
[6] P. Pyykko, *Chem. Rev.*, 1997, **97**, 597.
[7] F. Rabilloud, *J. Comput. Chem.*, 2012, **33**, 2083–2091.
[8] S. Lecoultre, A. Rydlo, C. Félix, J. Buttet, S. Gilb and W. Harbich, *J. Chem. Phys.*, 2011, **134**, 074302.
[9] F. Rabilloud, *J. Phys. Chem. A*, 2013, **117**, 4267–4278.
[10] J. Tiggesbumker, L. Kller, H. O. Lutz and K. H. Meiwes-Broer, *Chem. Phys. Lett.*, 1992, **190**, 42.
[11] J. Tiggesbaumker, L. Koller, K. H. Meiwes Broer and A. Liebsch, *Phys. Rev. A*, 1993, **48**, R1749–52.
[12] W. Harbich, S. Fedrigo and J. Buttet, *Chem. Phys. Lett.*, 1992, **195**, 5–6.
[13] S. Fedrigo, W. Harbich and J. Buttet, *Phys. Rev. B*, 1993, **47**, 10706–10715.
[14] M. Harb, F. Rabilloud, D. Simon, A. Rydlo, S. Lecoultre, F. Conus, V. Rodrigues and C. Félix, *J. Chem. Phys.*, 2008, **129**, 194108.
[15] S. Lecoultre, A. Rydlo, J. Buttet, C. Félix, S. Gilb and W. Harbich, *J. Chem. Phys.*, 2011, **134**, 184504.
[16] K. Baishya, J. C. Idrobo, S. Ogut, M. Yang, K. Jackson and J. Jullinek, *Phys. Rev. B*, 2008, **78**, 075439.
[17] M. Tiago, J. Idrobo, S. Ogut, J. Jellinek and J. Chelikowsky, *Phys. Rev. B*, 2009, **79**, 155419.
[18] M. Harb, F. Rabilloud and D. Simon, *Chem. Phys. Lett.*, 2009, **476**, 186–190.
[19] D. W. Silverstein and L. Jensen, *J. Chem. Phys.*, 2010, **132**, 194302.
[20] H. C. Weissker and C. Mottet, *Phys. Rev. B*, 2011, **84**, 165443.
[21] F. Rabilloud, *Eur. Phys. J. D*, 2013, **67**, 18.
[22] M. E. Casida, *in Recent Advances in Density Functional Methods. Part I, p. 155*, D.P. Chong Ed. (Singapore, World Scientific), 1995.
[23] E. Runge and E. K. U. Gross, *Phys. Rev. Lett.*, 1984, **52**, 997–1000.
[24] R. van Leeuwen, *Int. J. Mod. Phys. B*, 2001, **15**, 1969–2023.

[25] B. A. Collings, K. Athanassenas, D. Lacombe, D. M. Rayner and P. A. Hackett, *J. Chem. Phys.*, 1994, **101**, 3506.

[26] S. Gilb, K. Jacobsen, D. Schooss, F. Furche, R. Ahlrichs and M. M. Kappes, *J. Chem. Phys.*, 2004, **121**, 4619–4627.

[27] A. N. Gloess, H. Scneider, J. M. Weber and M. M. Kappes, *J. Chem. Phys.*, 2008, **128**, 114312.

[28] H. Hakkinen, B. Y. nad U. Landman, X. Li, H. J. Zhai and L. S. Wang, *J. Phys. Chem. A*, 2003, **107**, 6168–6175.

[29] S. M. Lang, P. Claes, N. T. Cuong, M. T. Nguyen, P. Lievens and E. Janssens, *J. Chem. Phys.*, 2011, **135**, 224305.

[30] A. Shayeghi, R. L. Johnston and R. Schafer, *Phys. Chem. Chem. Phys.*, 2013, **15**, 19715–19723.

[31] K. R. Geethalakshmi, F. Ruiperez, S. Knecht, J. M. Ugalde, M. D. Morse and I. Infante, *Phys. Chem. Chem. Phys.*, 2012, **14**, 8732–8741.

[32] A. Castro, M. A. Marques, A. H. Romero, M. J. Oliveira and A. Rubio, *J. Chem. Phys.*, 2008, **129**, 144110.

[33] J. C. Idrobo, W. Walkosz, S. F. Yip, S. Ogut, J. Wang and J. Jellinek, *Phys. Rev. B*, 2007, **76**, 205422.

[34] X. Lopez-Lozano, C. Mottet and H. C. Weissker, *J. Phys. Chem. C*, 2013, **117**, 3062–3068.

[35] N. Durante, A. Fortunelli, M. Broyer and M. Stener, *J. Phys. Chem. C*, 2011, **115**, 6277–6282.

[36] J. V. Koppen, M. Hapka, M. M. Szczesniak and G. Chalasinski, *J. Chem. Phys.*, 2012, **137**, 114302.

[37] S. Lecoultre, A. Rydlo, C. Félix, J. Buttet, S. Gilb and W. Harbich, *J. Chem. Phys.*, 2011, **134**, 074303.

[38] K. Baisha, J. C. Idrobo, S. Ogut, M. Yang, K. Jackson and J. Jullinek, *Phys. Rev. B*, 2011, **83**, 245402.

[39] T. Yasuike and K. Nobusada, *Phys. Chem. Chem. Phys.*, 2013, **15**, 5424–5429.

[40] T. Leininger, H. Stoll, H. J. Werner and A. Savin, *Chem. Phys. Lett.*, 1997, **275**, 151–160.

[41] H. Iikura, T. Tsuneda, T. Yanai and K. Hirao, *J. Chem. Phys.*, 2001, **115**, 3540–3544.

[42] D. Andrae, U. Haussermann, M. Dolg, H. Stoll and H. Preuss, *Theor. Chim. Acta*, 1990, **77**, 123–141.

[43] F. Weigend and R. Ahlrichs, *Phys. Chem. Chem. Phys.*, 2005, **7**, 3297–3305.

[44] Y. Zhao and D. G. Truhlar, *J. Chem. Phys.*, 2006, **125**, 194101.

[45] T. Yanai, D. P. Tew and N. C. Handy, *Chem. Phys. Lett.*, 2004, **393**, 51–57.

[46] A. D. Becke, *J. Chem. Phys.*, 1993, **98**, 5648–5652.

[47] P. J. Stephens, F. J. Devlin, C. F. Chabalowski and M. J. Frisch, *J. Phys. Chem.*, 1994, **98**, 11623–11627.

[48] M. J. Frisch, G. W. Trucks, H. B. Schlegel, G. E. Scuseria, M. A. Robb, J. R. Cheeseman, G. Scalmani, V. Barone, B. Mennucci, G. A. Petersson, H. Nakatsuji, M. Caricato, X. Li, H. P. Hratchian, A. F. Izmaylov, J. Bloino, G. Zheng, J. L. Sonnenberg, M. Hada, M. Ehara, K. Toyota, R. Fukuda, J. Hasegawa, M. Ishida, T. Nakajima, Y. Honda, O. Kitao, H. Nakai, T. Vreven, J. A. Montgomery, Jr., J. E. Peralta, F. Ogliaro, M. Bearpark, J. J. Heyd, E. Brothers, K. N. Kudin, V. N. Staroverov, R. Kobayashi, J. Normand, K. Raghavachari, A. Rendell, J. C. Burant, S. S. Iyengar, J. Tomasi, M. Cossi, N. Rega, J. M. Millam, M. Klene, J. E. Knox, J. B. Cross, V. Bakken, C. Adamo, J. Jaramillo, R. Gomperts, R. E. Stratmann, O. Yazyev, A. J. Austin, R. Cammi, C. Pomelli, J. W. Ochterski, R. L. Martin, K. Morokuma, V. G. Zakrzewski, G. A. Voth, P. Salvador, J. J. Dannenberg, S. Dapprich, A. D. Daniels, A. Farkas, J. B. Foresman, J. V. Ortiz, J. Cioslowski and D. J. Fox, *Gaussian 09 Revision B.01*, Gaussian Inc. Wallingford CT 2010.

[49] A. R. Allouche, *J. Comput. Chem.*, 2011, **32**, 174–182.

[50] V. K. M. Itoh, T. Adschiri and Y. Kawazoe, *J. Chem. Phys.*, 2009, **131**, 174510.

[51] M. Jiang, Q. Zeng, T. Zhang, M. Yang and K. A. Jackson, *J. Chem. Phys.*, 2012, **136**, 104501.

[52] G. Zanti and D. Peeters, *Theor. Chem. Acta*, 2013, **132**, 1300.

[53] G. te Velde, F. Bickelhaupt, E. Baerends, C. F. Guerra, S. van Gisbergen, J. Snijders and T. Ziegler, *J. Comput. Chem.*, 2001, **22**, 931–967.

[54] E. B. E. van Lenthe and J. Snijders, *J. Chem. Phys.*, 1994, **101**, 9783.

[55] J. S. E. van Lenthe and E. Baerends, *J. Chem. Phys.*, 1996, **105**, 6505.

[56] P. R. T. Schipper, O. V. Gritsenko, S. J. A. van Gisbergen and E. J. Baerends, *J. Chem. Phys.*, 2000, **112**, 1344.

[57] M. Harb, F. Rabilloud and D. Simon, *J. Chem. Phys.*, 2009, **131**, 174302.

[58] R. Fournier, *J. Chem. Phys.*, 2001, **115**, 2165–2177.

[59] C. Sieber, J. Buttet, W. Harbich and C. Félix, *Phys. Rev. A*, 2004, **70**, 041201(R).

[60] J. V. Koppen, M. Hapka, M. M. Szczesniak and G. Chalasinski, *J. Chem. Phys.*, 2012, **137**, 114302.

[61] C. M. Aikens and G. C. Schatz, *J. Phys. Chem. A*, 2006, **110**, 13317–13324.

[62] A. Rubio and L. Serra, *Phys. Rev. B*, 1993, **48**, 18222–18229.

[63] L. Jensen, L. L. Zhao and G. C. Schatz, *J. Phys. Chem. C*, 2007, **111**, 4756–4764.

[64] B. Gervais, E. Giglio, E. Jacquet, A. Ipatov, P.-G. Reinhard, F. Fehrer and E. Suraud, *J. Chem. Phys.*, 2004, **121**, 8466–8480.

[65] B. Gervais, E. Giglio, E. Jacquet, A. Ipatov, P.-G. Reinhard, F. Fehrer and E. Suraud, *Phys. Rev. A*, 2005, **71**, 015201.